J Appl Electrochem (2007) 37:1191–1200
DOI 10.1007/s10800-007-9386-1

ORIGINAL PAPER

Effect of sulfur-containing amino acids on the corrosion of mild steel in sulfide-polluted sulfuric acid solutions

M. S. Morad

Received: 27 February 2007 / Revised: 21 July 2007 / Accepted: 23 July 2007 / Published online: 16 August 2007

Abstract The influence of cysteine (RSH) and cystine (RSSR) on the corrosion behavior of mild steel in sulfide-polluted H_2SO_4 solutions was studied by potentiodynamic polarization methods and AC impedance technique. The results show that S^{2-} accelerates the corrosion process markedly, especially the anodic dissolution of iron. Tafel polarization curves show that RSH and RSSR act mainly as anodic-type inhibitors without affecting the mechanism of the hydrogen evolution reaction or iron dissolution. Adsorption of RSH and RSSR in most sulfide-polluted H_2SO_4 solutions obeys Temkin's isotherm. Impedance studies indicate that in the inhibited and uninhibited solutions, charge transfer controls the corrosion process either at E_{corr} or at 30 mV vs E_{corr}. Potentiodynamic anodic polarization curves show that RSSR effectively inhibits the steel dissolution both in the active and passive states and greatly reduces the current oscillations observed in the passive region.

Keywords Adsorption · Amino acids · Corrosion inhibition · Current oscillations · H_2S corrosion

1 Introduction

The corrosion of steel by H_2S is a significant problem in oil refineries and natural gas treatment facilities and can occur at all stages of production, from down hole to surface processing equipment. The capital and operational expenditures and health, safety, and environment of the oil and gas industry are enormously affected by corrosion. The presence of H_2S in fluids makes for a very aggressive environment which leads to severe corrosion of mild steel which still constitutes an estimated 99% of the pipeline material used in the oil and gas industry [1].

Research in sulfuric acid media has shown that the presence of sulfide ions (S^{2-}) or hydrogen sulfide (H_2S) is very aggressive towards many metals, particularly iron, nickel and stainless steel. The effect of S^{2-} on iron has been particularly studied. The intensification is attributable to the formation of ferrous sulfide (FeS) which is soluble in H_2SO_4 or the specific adsorption of HS^- ions [2].

The anodic dissolution of Fe in H_2SO_4 solutions containing H_2S was studied using steady-state polarization curves and the ac impedance technique. The results showed that H_2S markedly accelerates both the anodic dissolution of Fe and cathodic hydrogen evolution in most cases, but it can also exhibit a strong inhibiting effect upon Fe dissolution under certain conditions ($[H_2S] < 0.04$ mM, pH = 3–5 [3]. To verify the inhibitive action of H_2S, Ma et al. [4] further studied the influence of H_2S on the corrosion of iron in H_2SO_4/Na_2SO_4 solutions of different pH (pH = 0.75–3.5). The effect of H_2S was found to be related to the formation of a protective FeS film at the iron surface. The inhibiting effect of FeS was explained by the formation of a metastable mackinwite (one of the crystalline form of FeS) that converts to troilite and pyrite with greater stability and protective properties.

Most of the inhibitors currently used in the gas industry to protect pipelines for collection and transport of wet H_2S-containing gas are nitrogen—containing compounds, in particular, amines and their derivatives [5–9], Schiff bases containing different azomehine groups [10] and imidazoline derivatives [11]. These inhibitors [5–11] have been tested in weakly acidic and neutral media.

M. S. Morad (✉)
Electrochemistry research laboratory, Department of Chemistry, Faculty of Science, Assiut University, Assiut 71516, Egypt
e-mail: morad60@acc.aun.edu.eg; mmorad04@yahoo.com

Amino acids have been successfully used as corrosion inhibitors in many practical applications [12, 13]. To the best of our knowledge, no data are available in the literature on the use of amino acids as inhibitors for the corrosion of mild steel in H_2SO_4 containing H_2S. In this work, S-containing amino acids, namely, cysteine (RSH) and cystine (RSSR) were tested. Preliminary experiments showed that S-free amino acids accelerate mild steel corrosion in H_2SO_4/H_2S solution. RSH (which contains one sulfur atom) and its oxidized form RSSR (which contains two sulfur atoms) were chosen to explore the role of the number of sulfur atoms on the adsorption of the amino acid on the steel surface covered with HS^- ions and at the same time to investigate the possibility of the use of these eco-friendly compounds as inhibitors for the corrosion of mild steel in such aggressive environments. Both potentiodynamic polarization curves and the impedance (EIS) technique were used.

2 Experimental section

Electrochemical studies were carried out in a three electrode cell. A mild steel cylinder, whose composition is given elsewhere [12], pressed in a Teflon holder, acted as a working electrode. Its working area was 0.196 cm^2. A saturated calomel electrode (SCE) and a platinum sheet of large surface area served as reference and auxiliary electrodes, respectively.

Prior to each experiment the working electrode was wet polished with emery paper up to grade 600, rinsed with bi-distilled water, acetone, bi-distilled water and transferred wet to the glass cell, already filled with 200 ml of 1 M H_2SO_4 solution. The latter was deaerated by purified nitrogen for 1 h prior to insertion of the working electrode; purging with nitrogen continued during the course of the experiments. All experiments were carried out after 30 min of exposure in the solution. The temperature of the electrolyte was 40 ± 0.2 °C.

EG&G instruments electronic equipment was used. It included a PAR Model 273 potentiostat/galvanostat and a 5210 two-phase lock-in analyzer. Steady-state polarization curves (Tafel plots) were conducted with a scan rate of 0.2 mV s^{-1} in the potential range −200 to +125 mV from the corrosion potential (E_{corr}). For the potentiodynamic anodic polarization curves, the scan rate was 5 mV s^{-1} and the potential range was −100 to +2,500 mV vs E_{corr}. H_2SO_4 solutions containing 50 and 1,000 ppm S^{2-} were used while 1×10^{-2} M RSH and 5×10^{-3} M RSSR were tested.

EIS measurements were taken from 100 μHz to 100 kHz. The response of the electrochemical system to ac excitations with a frequency ranging mainly from 631 kHz to 0.1 Hz and a peak to peak ac amplitude of 5 mV with 5 points per decade. Impedance spectra were recorded at E_{corr} and +30 mV with respect to E_{corr}.

Both polarization curves and impedance measurements were monitored by an IBM personal computer via a GBIP-IIA interface. The standard programs M352/252 and M398 were used for collecting the experimental data.

1 M H_2SO_4 solution was prepared from concentrated H_2SO_4 (Merck) and bi-distilled water. Sulfide ion was tested in the concentration range 50–1,000 ppm by addition of $(NH_4)_2S$ (Merck) to H_2SO_4 solution. Both RSH (Aldrich) and RSSR (Merck) were used without further purification. All experiments were conducted in stagnant solutions.

3 Results and discussion

3.1 Open-circuit corrosion potentials (E_{corr})

The open-circuit corrosion potentials (E_{corr}) of the system: mild steel/H_2SO_4 + S^{2-} in the absence and presence of 1×10^{-4}–1×10^{-2} M RSH are shown in Fig. 1. In the absence of RSH, values of E_{corr} are shifted in the negative direction with increasing sulfide ion concentration. The negative shift of E_{corr} can be attributed to the adsorption of HS^- ions on the steel surface which leads to activation of the corrosion process.

In the presence of RSH, values of E_{corr} are more noble than those of the blank solution. The positive shift of E_{corr} is increased with increasing RSH concentration reaching its maximum value at 1×10^{-2} M. This behavior can be attributed to the adsorption of RSH on the anodic sites of the surface and RSH can be considered as an inhibitor of anodic type (see below). RSSR showed the same behavior with the difference that the positive shift (ΔE) in the case

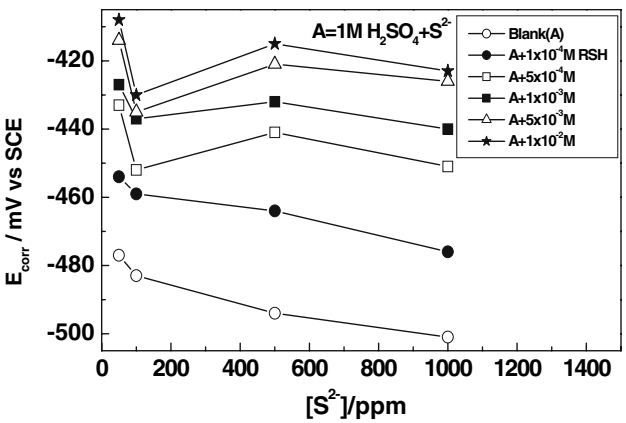

Fig. 1 Influence of S^{2-} concentration the corrosion potential of mild steel M H_2SO_4 solution without and with RSH at 40°C

of RSSR is more pronounced than that of RSH for the same sulfide ion concentration. For example, in H_2SO_4 containing 1,000 ppm S^{2-} and in the presence of the maximum examined concentration (1×10^{-2} M RSH, 5×10^{-3} M RSSR), values of ΔE were found to be 35 and 56 mV for RSH and RSSR, respectively.

3.2 Tafel polarization curves

The polarization curves of mild steel traced in sulfuric acid without and with 50–1,000 ppm S^{2-} are shown in Fig. 2. The anodic branch of the polarization curve recorded in H_2SO_4 alone is notably moved towards higher current density values while the cathodic branch remains approximately unaffected. This means that the accelerating effect of S^{2-} on the anodic dissolution reaction of iron is stronger than on the hydrogen evolution reaction, making the corrosion potential move to the negative direction. This result agrees with that obtained for the effect of H_2S on the corrosion behavior of Cr in H_2SO_4/Na_2SO_4 solution of pH 2 [14]. The overall corrosion current density (i_{corr}), which was calculated from the intersection of the linear portions (Tafel regions) of the anodic and cathodic arms at E_{corr}, is greatly enhanced. Although the accelerating action of sulfide ion, values of the anodic (β_a) and cathodic ($-\beta_c$) Tafel slopes of the pure medium remain approximately unchanged. Values of β_a ranged from 48 to 65 mV/decade while those of β_c have a mean value of −110 mV/decade. The results suggest that the presence of S^{2-} has no influence on the mechanism of hydrogen evolution reaction (her) or the iron dissolution.

Figure 3 shows the influence of 5×10^{-5}–5×10^{-3} M RSSR on the polarization curves recorded in H_2SO_4 solution containing 1,000 ppm S^{2-}. The presence of RSSR has little influence on the cathodic polarization curve of the blank solution while the anodic curve is largely shifted towards lower current densities. Thus, RSSR can be considered as an anodic inhibitor. On the other hand, the presence of RSSR has no influence on the value of β_c of the blank solution while β_a decreases slightly and reaches a value of 35 mV/decade which is nearly the same as the theoretical value of β_a for iron dissolution (30 mV/decade). Therefore, the presence of RSSR has no influence on the mechanism of hydrogen evolution or iron dissolution and the inhibition process occurs by adsorption (simple surface coverage).

Values of i_{corr} obtained in the presence of RSSR are lower than that of the blank solution and the lowest value of i_{corr} is obtained in the presence of 5×10^{-3} M RSSR. RSH showed the same behavior.

Values of i_{corr} were used to calculate the inhibition efficiency (IE%) as follows

$$\text{IE\%} = [(i^{o}_{corr} - i_{corr})/i^{o}\text{corr}] \times 100 \quad (1)$$

where i°_{corr} and i_{corr} are the corrosion current density obtained in the absence and presence of the amino acid.

Values of IE% obtained in the presence of RSH and RSSR were plotted as a function of the additive concentration at different S^{2-} as shown in Figs. 4 and 5, respectively.

Figure 4 shows that in the solution containing the same S^{2-}, IE% increases with increasing concentration of RSH, reaching a maximum at the highest concentration of RSH (1×10^{-2} M). In H_2SO_4 solution containing 1×10^{-2} M RSH, the highest inhibition efficiency is obtained in the solution containing 100 ppm S^{2-} while the lowest is obtained in solution containing 1,000 ppm S^{2-}.

For RSSR (Fig. 5), in the solution containing the same S^{2-}, IE% increases with increasing concentration of RSSR reaching a maximum at 1×10^{-3} M and after that it

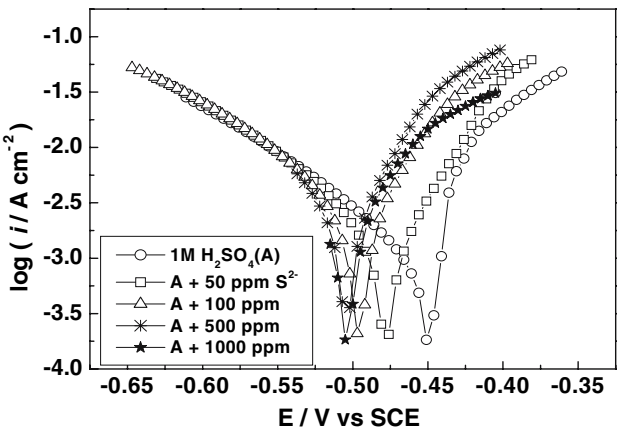

Fig. 2 Potentiodynamic polarization curves of mild steel in 1 M H_2SO_4 solution without and with different concentrations of S^{2-} ion

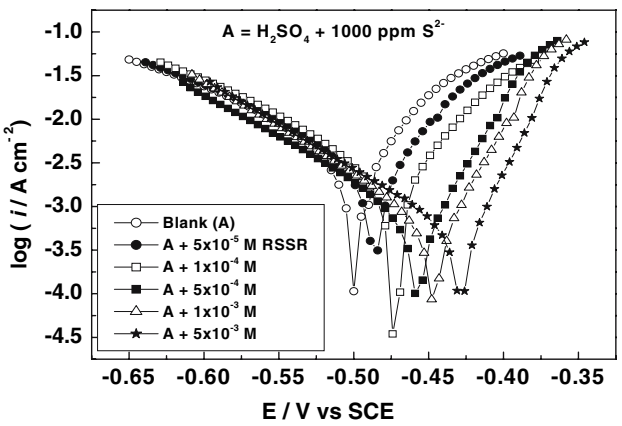

Fig. 3 Potentiodynamic polarization curves of mild steel in 1 M H_2SO_4 solution without and with RSSR in presence 1,000 ppm of S^{2-} ion

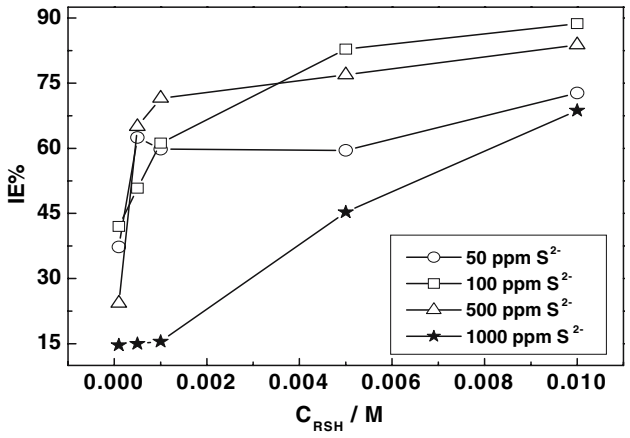

Fig. 4 Influence of S^{2-} concentration of the inhibition efficiency of RSH as calculated from Tafel plots

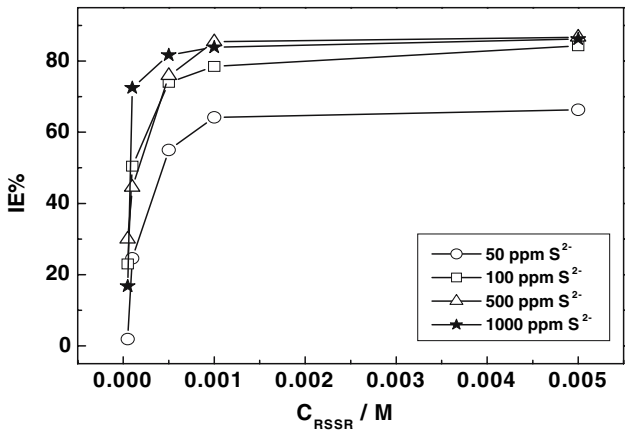

Fig. 5 Influence of S^{2-} concentration of the inhibition efficiency of RSSR as calculated from Tafel plots

remains unchanged. In the solution containing the highest concentration of RSSR (5×10^{-3} M), the lowest inhibition efficiency ($\sim$60%) is observed in the solution containing 50 ppm S^{2-} while in the remaining solutions the efficiency is approximately the same ($\sim$90%).

Figures 4 and 5 demonstrate that RSSR, as an inhibitor, performs better than RSH in H_2SO_4 solution containing S^{2-} ions. This may be attributed the presence of the two S atoms, which act as adsorption centers. These centers offer stronger adsorption for RSSR on the anodic sites of the surface than RSH, which has one S atom.

3.3 Adsorption isotherms

Adsorption of an inhibitor on a metal surface can affect the reaction kinetics either by decreasing the available surface area for corrosion (blocking effect) or by modifying the electrochemical standard Gibbs free energy of activation [15]. The decrease in the corrosion current density observed in the presence of RSH and RSSR with unchanged Tafel slopes suggest the possibility of calculating the degree of surface coverage (θ) according to the equation:

$$\theta = [(i^{o}_{corr} - i_{corr})/i^{o}corr] \quad (2)$$

In an attempt to find the best fit of θ values to various adsorption isotherms, it was found that the suitable isotherm depends on the sulfide ion concentration. Adsorption of RSH and RSSR obeys Temkin's isotherm (θ is a linear function of log C, where C is the concentration of the inhibitor in bulk solution) except in the solution containing 1,000 ppm S^{-2} for RSH and in the solution containing 50 ppm S^{-2} for RSSR. In the latter two cases, adsorption of RSH and RSSR follows Langmuir's isotherm (C/θ is a linear function of C). However, Figs. 6–8 show Temkin and Langmuir isotherms and were plotted according the following equations:

$$\text{Langmuir's isotherm:} \quad C/\theta = (1/K) + C \quad (3)$$

$$\text{Temkin's isotherm:} \quad \theta = (1/f)\ \ln KC \quad (4)$$

where f is the heterogeneity factor and K is the adsorption equilibrium constant, which is related to the standard free energy of adsorption (ΔG°_{ads}) by the equation:

$$K = (1/55.5)\ \exp\ (-\Delta G^{o}_{ads} / RT) \quad (5)$$

Equation 5 allows the calculation of ΔG°_{ads}. Values of K and ΔG°_{ads} were calculated and are given in Table 1. K ranges from 227.3 to 5.1×10^{12} M^{-1}. The high values of K

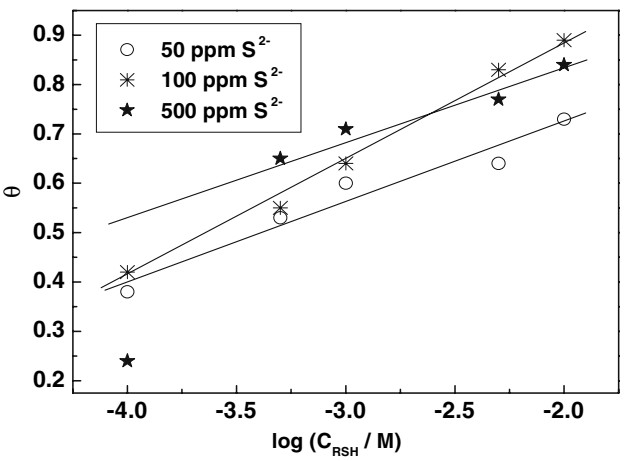

Fig. 6 Temkin adsorption isotherm of RSH on mild steel surface in 1 M H_2SO_4 solution containing different concentrations of S^{2-} ion

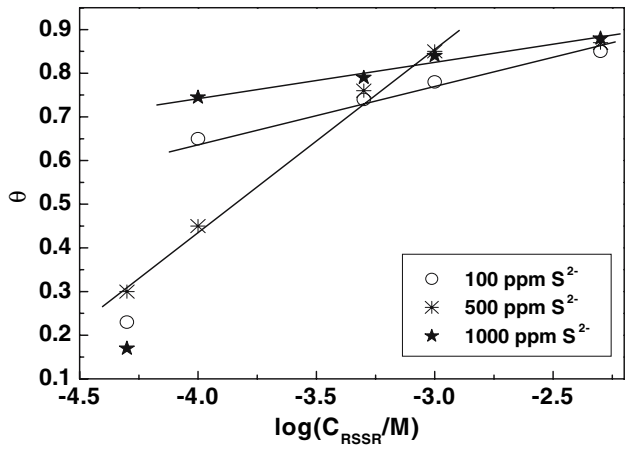

Fig. 7 Temkin adsorption isotherm of RSSR on mild steel surface in 1 M H_2SO_4 solution containing different concentrations of S^{2-}ion

indicate the strength of interaction between the adsorbed amino acids and the metal surface [16]. On the other hand, values of $\Delta G°_{ads}$ range from −24.5 to −86.5 kJ mol^{-1}. It was reported [17, 18] that values of $\Delta G°_{ads}$ of the order −20 kJ mol^{-1} or lower are generally consistent with physical adsorption while those above −40 kJ mol^{-1} involve chemisorption, that is, charge sharing or transfer from the inhibitor molecules to the metal surface, and coordinate type bonding. Values of $\Delta G°_{ads}$ between −20 kJ mol^{-1} and −40 kJ mol^{-1} indicate weak chemisorption. Based on these facts, RSH in the solution containing 1,000 ppm S^{2-} and RSSR in the solution containing 50 ppm S^{2-} are weakly chemisorbed on the steel surface. This may explain the low inhibition efficiency of RSH and RSSR in these solutions. In the remaining solutions, RSH and RSSR are strongly adsorbed (chemisorbed) on the steel surface and such adsorption imparts high inhibition efficiency.

Table 1 Parameters of adsorption of RSH and RSSR on mild steel surface in 1M H_2SO_4 solution containing different concentrations of S^{2-} ions

$[S^{2-}]$/ppm	RSH		RSSR	
	K/M^{-1}	$\Delta G°_{ads}$/kJ mol^{-1}	K/M^{-1}	$\Delta G°_{ads}$/kJ mol^{-1}
50	3.2×0^6	−49.3	5555	−32.8
100	4.6×10^5	−44.3	3.6×10^9	−67.6
500	1.7×10^8	−59.7	5.2×10^5	−44.6
1,000	227.3	−24.5	5.1×10^{12}	−86.5

3.4 Impedance measurements

3.4.1 Impedance behavior at the corrosion potential

The aim of this technique is to get more information concerning the electrochemical processes which occur at the mild steel/1M H_2SO_4 interface in the absence and presence of 50–1,000 ppm S^{2-} and the effect of both RSH and RSSR on these processes. For this purpose, impedance spectra in the form of Nyquist plots were recorded after 30 min immersion in 1M H_2SO_4 solution without and with 50–100 ppm S^{2-}.

The spectra (not shown here) have approximately the same shape, that is, one depressed capacitive loop which covers the frequency range 100 kHz to 0.398 Hz, followed by a small inductive loop. The inductive loop is commonly associated with a relaxation process of the adsorbed species at the metal/solution interface. The capacitive loop can be ascribed to charge transfer. In the presence of S^{2-}, the diameter of the capacitive loop of the pure acid solution was found to decrease with increasing concentration of sulfide ion (corrosion acceleration) while the inductive loop become more pronounced (more intermediate species are adsorbed on the steel surface). In all cases, the presence of S^{2-} did not affect the shape of the impedance spectra which indicates that charge transfer still controls the corrosion process. To interpret the impedance results and to chose the most suitable equivalent circuit, the non-linear least square (NLLS) fitting procedure developed by Boukamp [19] was used.

For all systems, the most suitable equivalent circuit consists of a solution resistance R_s in series with a parallel circuit of resistance of charge transfer R_{ct} and constant phase element related to the double-layer capacity Q_{dl}, that

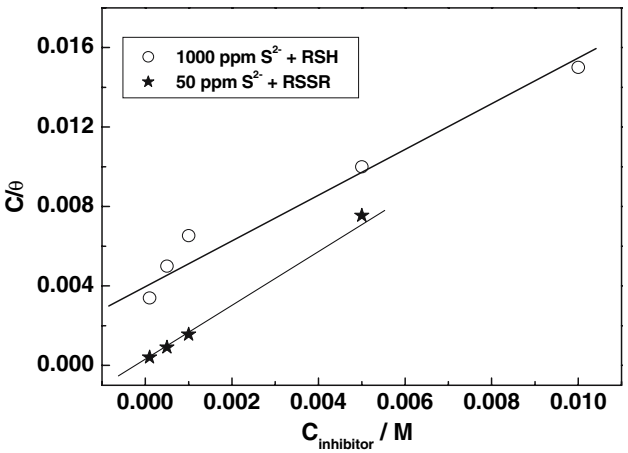

Fig. 8 Langmuir adsorption isotherm of RSH and RSSR on mild steel surface in 1 M H_2SO_4 solution in presence of certain concentrations of S^{2-}ion

is $R_s(R_{ct}\ Q_{dl})$. The latter element was used to overcome the frequency dispersion behavior which results from surface roughness, impurities, dislocations, grain boundaries, fractality, and distribution of the active centers, inhibitor adsorption, and the formation of porous layers [20].

The impedance of the constant phase element is given by the expression:

$$Z_{Qdl} = A^{-1}(j\omega)^{-n} \quad (6)$$

where A is a proportional factor while ***n*** is the phase shift [20]. It is seen that at ***n*** = 1, Q_{dl} gives pure capacitance behavior whose impedance function is:

$$Z_{Cdl} = (j\omega C)^{-1} \quad (7)$$

Values of R_{ct} and Q_{dl} obtained in sulfide-free H_2SO_4 solution were found to be 14.4 Ω cm^2 and 8.2×10^{-4} s^n Ω^{-1} cm^{-2} with an exponent ***n*** value of 0.95 respectively. In the presence of 50–1,000 ppm S^{2-}, the value of R_{ct} of the pure solution was found to decrease with increasing sulfide ion concentration, reaching a value of 6.5 Ω cm^2 at 1,000 ppm S^{2-} which means ~122% corrosion acceleration. Regarding the values of Q_{dl} and ***n***, it was found that addition of 50 ppm S^{2-} increases the value of Q_{dl} to 1.73×10^{-3} s^n Ω^{-1} cm^{-2} and reduces the value of ***n*** to 0.90.The latter values remained approximately unchanged regardless of the S^{2-} concentration. The increase in Q_{dl} and the decrease in ***n*** reflect the accelerating effect of sulfide ion towards mild steel corrosion in H_2SO_4.

Figure 9 is a representative example for the effect of RSH and RSSR on the impedance behavior of mild steel in sulfide-polluted sulfuric acid solution. It shows the influence of $1 \times 10^{-4} - 1 \times 10^{-2}$ M RSH on Nyquist plots of mild steel in H_2SO_4 solution containing 50 ppm S^{2-} recorded at E_{cor}. The Nyquist plots comprise one capacitive loop and the diameter of the loop increases with increasing additive concentration indicating its inhibition effect. As the addition of RSH has no effect on the shape of the impedance spectra, the equivalent circuit $R_s(R_{ct}\ Q_{dl})$ represents these systems and charge transfer controls the corrosion process. RSSR showed the same behavior. Values of the elements of suggested equivalent circuit were calculated and those of R_{ct} obtained in the presence of RSH in the presence of different sulfide ion concentrations are given in Table 2. Values of R_{ct} generally increase with increasing RSH concentration indicating its inhibitive action in sulfide-polluted H_2SO_4 solutions.

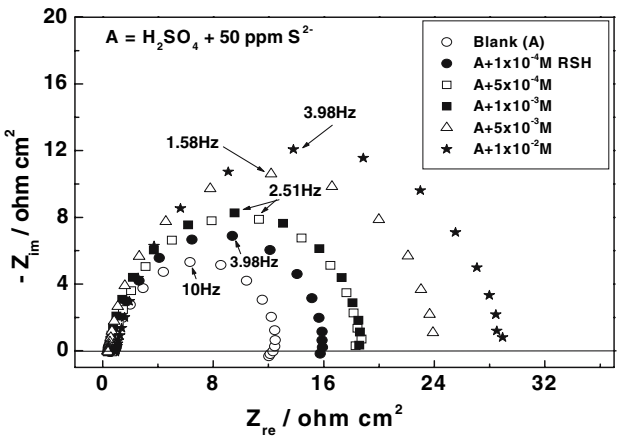

Fig. 9 Influence of RSH on Nyquist plot obtained for the corrosion of mild steel at E_{corr} in 1 M H_2SO_4 solution containing 50 ppm S^{2-}ion

Values of R_{ct} obtained in the presence of RSH and RSSR were used to calculate the inhibition efficiency of the additives using the following equation:

$$IE\% = \{ [R_{ct} - R^o_{ct}]/R_{ct} \} \times 100 \quad (8)$$

where R^o_{ct} and R_{ct} are charge transfer resistance obtained in the absence and presence of the amino acid.

Figures 10 and 11 show the dependence of IE% of RSH and RSSR on their concentrations in the presence of various concentrations of sulfide ion. For RSH, in H_2SO_4 solutions containing 50 –1,000 ppm S^{2-}, values of IE% (Fig. 10) increase with increase in RSH concentration. The best performance of RSH is in H_2SO_4 solutions containing 500 ppm S^{2-}. Figure 11 shows that IE% of RSSR increase with increasing additive concentration up to 1×10^{-3} M and then remain approximately unchanged. Accordingly, the inhibition efficiency of RSH and RSSR calculated from R_{ct} values agrees reasonably with that obtained from the polarization curves.

3.4.2 *Impedance behavior at 30 mV from the corrosion potential*

The impedance spectra for mild steel in 1M H_2SO_4 solutions containing 500 ppm S^{2-} in the absence and presence of 5×10^{-5}–5×10^{-3} M RSSR are shown in Fig. 12.

Table 2 Values of charge transfer resistance R_{ct} of mild steel corrosion in sulfide-polluted sulfuric acid solutions calculated from Nyquist plots recorded at E_{corr} in absence and presence of RSH

Additive	$[S^{2-}]$ / ppm			
	50	100	500	1,000
Blank	12	8.1	6.7	6.5
1×10^{-4}M RSH	15.3	11.7	9	6.9
5×10^{-4}M	18.1	13.7	15.4	7.3
1×10^{-3}M	18.4	14.8	18	7
5×10^{-3}M	23.6	23.1	19.4	10.3
1×10^{-2}M	28.1	28.9	26.6	16.7

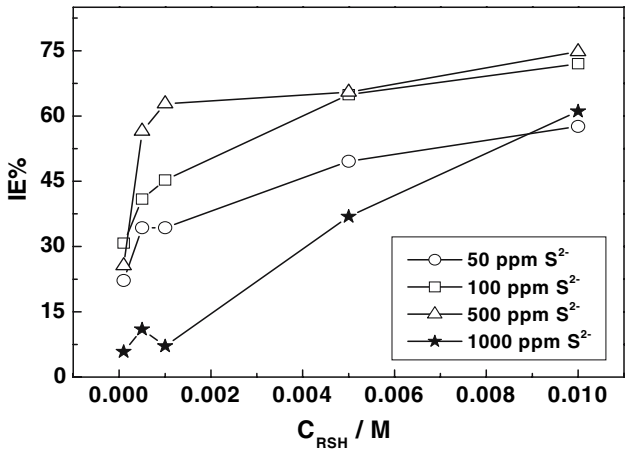

Fig. 10 Influence of S^{2-} concentration of the inhibition efficiency of RSH as calculated from values of R_{ct} obtained at E_{corr}

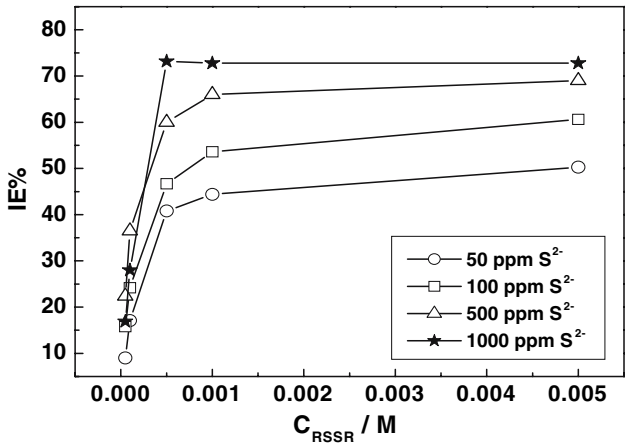

Fig. 11 Influence of S^{2-} concentration of the inhibition efficiency of RSSR as calculated from values of R_{ct} obtained at E_{corr}

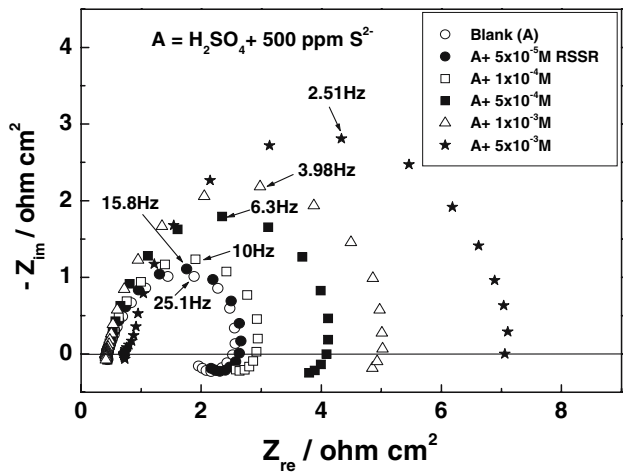

Fig. 12 Influence of RSSR on Nyquist plot obtained for the corrosion of mild steel at + 30 mV vs E_{corr} in 1M H_2SO_4 solution containing 500 ppm S^{2-}ion

These spectra were recorded at 30 mV more positive than E_{corr} (representative spectra). The Nyquist plot for the blank solution displays a high frequency capacitive loop followed by a small inductive loop at low frequency. Similarly to the results obtained at E_{corr}, the high-frequency capacitive loop indicates charge transfer resistance while the inductive loop at low frequency suggests the relaxation of adsorbed intermediates. In this regard, the adsorbed intermediate in sulfide-free H_2SO_4 solution is suggested to be FeOH species as a result of adsorption of H_2O molecules. As there is only one inductive loop, only one species is adsorbed.

In the presence of H_2S, the adsorption of H_2S molecules is much stronger than that of H_2O molecules. So, we can ignore the adsorption of H_2O and the H_2S molecules participate in the dissolution process [3]. In the presence of H_2S, a reaction model [3] is proposed to explain the appearance of the high-frequency capacitive loop and low-frequency inductive loop:

$$Fe + H_2S + H_2O \Leftrightarrow (FeSH)_{ads} + H_3O^+ + e \quad (9)$$

$$(FeSH)_{ads} \rightarrow FeSH^+ + e \quad (10)$$

$$FeSH^+ + H_3O^+ \Leftrightarrow Fe^{2+} + H_2S + H_2O \quad (11)$$

A reaction model similar to the above was proposed for the anodic dissolution of Cr in H_2S-containing H_2SO_4 solution [21].

Nyquist plots obtained in the presence of RSSR are characterized by the following features:

(a) The diameter of the capacitive loop increases with increasing cystine concentration indicating its inhibition effect.

(b) The capacitive loop is a perfect semicircle as indicated from the value of ***n*** where values of ***n*** obtained at all concentrations of cystine were found to be 1. The equivalent circuit representing the corrosion behavior at the corrosion potential represents the behavior under anodic polarization potential with the replacement of the constant phase element Q_{dl} by the capacity of the double layer C_{dl}. Accordingly, the equivalent circuit representing the interface at 30 mV more positive than E_{corr} is $R_s(R_{ct}\ C_{dl})$.

(c) The low-frequency inductive loop gradually disappears as the concentration of cystine increases and vanishes completely at 5×10^{-3} M cystine. The gradual disappearance of this loop indicates the displacement of HS^- by inhibitor molecules and their adsorption on anodic sites.

Values of R_{ct} obtained in the presence of RSH and RSSR were plotted as a function of additive concentration in H_2SO_4 solution containing various concentrations of

sulfide ion and shown in Figs. 13 and 14 respectively. In general, the inhibition efficiency of both RSH and RSSR increases with increasing concentration regardless of the concentration of sulfide ion. The best inhibiting effect of RSH is observed in H_2SO_4/500 ppm S^{2-} whereas RSSR performs well in solutions containing 500 and 1,000 ppm S^{2-}. The impedance results obtained at 30 mV vs E_{corr}, i. e. in the active dissolution region, reveal that RSH is superior as an anodic inhibitor in comparison to RSSR.

4 Effect of RSH and RSSR on the active–passive behavior of mild steel in sulfide-polluted H_2SO_4 solutions

Figure 15(a) shows the characteristic log I/E curve of mild steel in 1M H_2SO_4 solution. There are three main potential (i)–(iii) where different electrochemical processes take

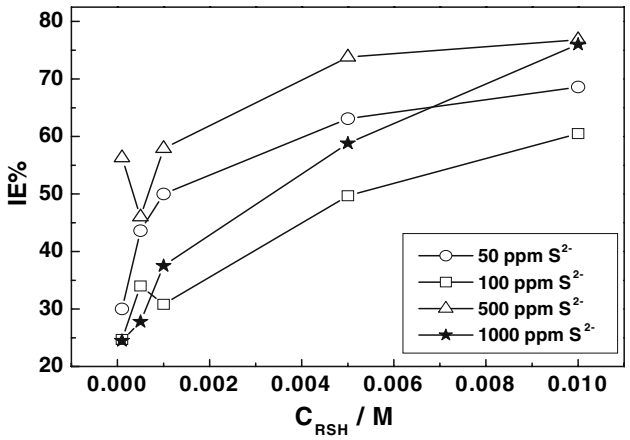

Fig. 13 Influence of S^{2-} concentration of the inhibition efficiency of RSH as calculated from values of R_{ct} obtained at + 30 mV vs E_{corr}

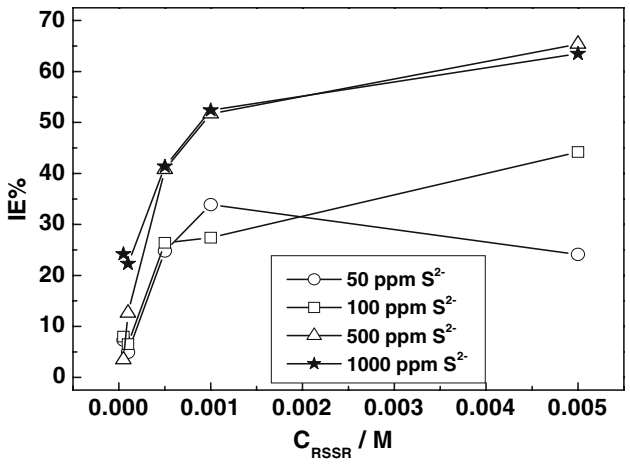

Fig. 14 Influence of S^{2-} concentration of the inhibition efficiency of RSSR as calculated from values of R_{ct} obtained at + 30 mV vs E_{corr}

place. Region (i) corresponds to the active state, where dissolution occurs from a bare iron surface. In region (ii), Fe dissolution occurs in the presence of a ferrous salt film. At the beginning of passive region (region iii), the passive current I_p, decreases dramatically due to coverage of the steel surface by a thin oxide film. Current oscillation appears in the passive region. Previous results for iron in H_2SO_4 [22], iron in $HClO_4$ [23], and X70 carbon steel in H_3PO_4 [24, 25] indicated that current oscillations usually take place within a narrow potential range where the iron electrode is in transition from the prepassive (region ii) to the passive state. According to [23], the origin of current oscillations is explained as follows: when current oscillations begin, Fe^{2+}, produced by the electrodissolution of iron according to BDD mechanism, will lead to the H^+ electromigration away from the vicinity of the iron electrode. In that case, $Fe(OH)_2$ probably precipitates as the initial surface blocking layer. This non-compact $Fe(OH)_2$ layer provides a locally high pH region that assists formation of a very thin, compact and temporarily stable Fe_2O_3 layer. Subsequently, the back diffusion of H^+ from the bulk solution to the interface causes dissolution of $Fe(OH)_2$ and Fe_2O_3 as a result of lowered pH at the interface. The appearance of the current oscillations over a relatively wide potential range ($\sim$400 mV) in the passive region may be ascribed to the fact that back diffusion of H^+ from the bulk solution to the interface occurs at more positive potential.

The influence of 1,000 ppm S^{2-} on the active–passive behavior of mild steel in H_2SO_4 solution is shown in Fig. 15b while the effect of 5×10^{-3}M RSSR on the active–passive behavior of mild steel in sulfide-polluted sulfuric acid is show in Fig. 15c (representative examples). Passivation parameters associated with Figs. 15a–c are given in Table 3. Although the presence of S^{2-} did not affect the general features of the anodic curve of the blank solution, the oscillatory amplitudes of current oscillations (Fig. 15b) are less intense in comparison with those observed in the blank solutions. Current oscillations are greatly reduced upon addition of 5×10^{-3} M RSSR (Fig. 15c) as a result of adsorption of RSSR on the anodic sites which prevents the dissolution of Fe^{2+} and hence the backward diffusion of H^+ from the bulk solution to the interface.

The results of Table 3 indicate that in the presence of 1,000 ppm S^{2-}, values of E_{pp} and E_{cp} obtained in H_2SO_4 are shifted positively, while values of I_{cc} and I_p increase.

So, sulfide ion accelerates the anodic dissolution of mild steel in both active and passive regions. On the other hand, in sulfide-polluted sulfuric acid solution, values of E_{pp} and E_{cp} obtained in the presence of RSSR shift in the negative direction while those of I_{cc} and I_p are reduced remarkably. These findings indicate the inhibition effect of RSSR towards the anodic dissolution of mild steel in both active

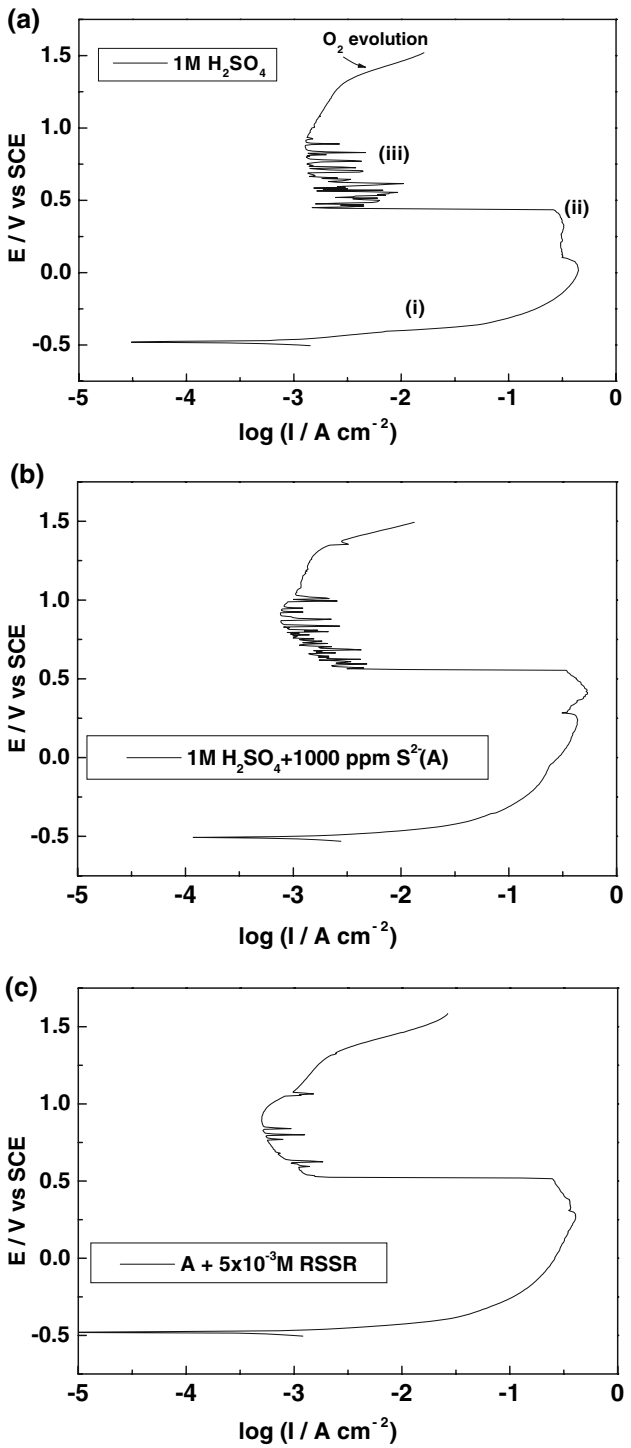

Fig. 15 Influence of RSSR on the active–passive behavior of mild steel in 1M H_2SO_4 solution containing 1000 ppm S^{2-}ion

and passive regions. The behavior of RSSR in H_2SO_4 containing 50 ppm S^{2-} is similar to that obtained in H_2SO_4 containing 1,000 ppm S^{2-} except that reduction of the current fluctuations is not as marked as that in the presence of 1,000 ppm S^{2-}.

Table 3 Effect of RSSR on the anodic polarization characteristics of mild steel in 1M H_2SO_4 solution containing 1,000 ppm S^{2-} ions

	E_{pp}/mV	I_{cc}/mA cm^{-2}	E_{cp}/mV	I_p/μA cm^{-2}	Passive range/mV
1 M H_2SO_4	38	451	455	1660	480
1,000 ppm S^{2-}	409	544	555	3605	480
5×10^{-3}M RSSR	269	421	541	1288	435

The effect of RSH on the active–passive behavior of mild steel in sulfide-polluted sulfuric acid is similar to that obtained in the presence of RSSR except that RSH could not prevent current oscillations in the passive region. This may be ascribed to the fact that the adsorption of RSH is not so strong as that of RSSR because it contains only one adsorption center, that is one sulfur atom.

5 Conclusions

The main conclusions drawn from this study are:

- The presence of 50–1,000 ppm S^{2-} remarkably enhances the corrosion of mild steel in 1 M H_2SO_4 solution. The anodic dissolution of Fe is much more affected than the cathodic hydrogen evolution reaction (her).
- RSH and RSSR have been found to perform as well in sulfide-polluted H_2SO_4 solutions. A better performance is noticed in the case of RSSR. The presence of RSH and RSSR has no influence on the mechanism of her or iron dissolution.
- Both RSH and RSSR are inhibitors of the anodic type and their adsorption on the steel surface in the most studied solutions follows Temkin's adsorption isotherm.
- Charge transfer controls the corrosion of mild steel in sulfide-polluted H_2SO_4 solutions without and with RSH and RSSR at E_{corr} and at 30 mV vs E_{corr}. At E_{corr}, the interface is represented by $R_e(R_{ct}\,Q_{dl})$ while at 30 mV vs E_{corr}, the interface is better represented by $R_e(R_{ct}\,C_{dl})$.
- RSSR effectively inhibits steel dissolution both in the active and passive states and greatly reduces the current oscillations in the passive region. RSH shows the same effect as RSSR but could not prevent current oscillations.

References

1. Parakala SR (2005) EIS investigation of carbon dioxide and hydrogen sulfide corrosion under film forming conditions, M. Sc. Thesis. Ohio University
2. Bellaouchou A, Guenbour A, Benbachir A (1993) Corrosion 49:656

3. Ma H, Cheng X, Chen S, Wang C, Zhang J, Yang H (1998) J Electroanal Chem 451:11
4. Ma H, Cheng X, Li G, Chen S, Quan Z, Zhao S, Niu L (2000) Corros Sci 42: 1669
5. Kuznestov YI, Vagapov RK (2002) Prot Met 38: 210
6. Murav'eva SA, Mel'nikov VG, Egorov VV (2003) Prot Met 39:468
7. Vigdorovich VI, Sinyutina SE, Tsygankova LE, Oshe EK (2004) Prot Met 40:264
8. Murav'eva SA, Mel'nikov VG (2005) Theor Found Chem Eng 39:81
9. Frolova LV, Tomina EV (2006) Prot Met 42:215
10. Kuznestov YI, Vagapov RK (2001 Prot Met 37:210
11. Galicia P, Gonzalez I (2005) Electrochim Acta 50:4451
12. Morad MS (2005) J Appl Electrochem 35: 889
13. Morad MS (2007) J Appl Electrochem 37:661
14. Cheng X, Ma H, Chen S, Niu L, Lei S, Yu R, Yao Z (1999) Corros Sci 41:773
15. Vracar Lj, Drazic DM (1992) J Electroanal Chem 33:269
16. Noor EA (2005) Corros Sci 47:33
17. Grubac Z, Babic R, Metikos-Hukovic M (2002) J Appl Electrochem 32:431
18. Tremont R, Cabrera CR (2002) J Appl Electrochem 32:783
19. Boukamp BA (1989) Equivalent circuit (EQUIVCRT, PAS), User's manual second version revised edition. University of Twente
20. Popova A, Raicheva S, Sokolova E, Christov M (1996) Langmuir 12: 2038
21. Cheng X, Ma H, Chen S, Niu L, Lei S, Yu R, Yao Z (1999) Corros Sci 41: 773
22. Pagitass M, Diamantopoulou A, Sazou D (2001) Electrochem Commun 3: 330
23. Ma H, Li G, Chen S, Zhao S, Cheng X (2002) Corros Sci 44:1177, and references therein
24. Bojinov M, Betova I, Fabricius G, Laitinen T, Raicheff R (1999) J Electroanal Chem 475: 58
25. Li L, Luo JL, Yu JG, Zeng YM, Lu BT, Chen SH (2003) Electrochem Commun 5:396